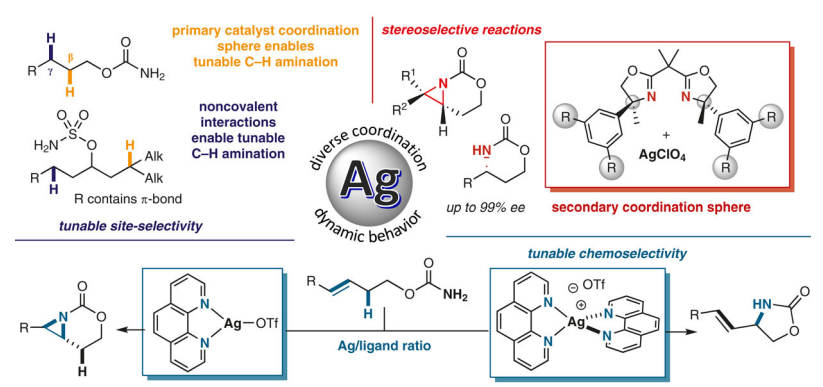
Logan E. Vine [⋄] Emily E. Zerull[®] [⋄] Jennifer M. Schomaker*[®]

University of Wisconsin, Department of Chemistry, 1101 University Avenue, Madison, WI 53706, USA schomakerj@chem.wisc.edu



Received: 29.05.2020 Accepted after revision: 12.06.2020 Published online: 29.07.2020 DOI: 10.1055/s-0040-1707197; Art ID: st-2020-a0323-a



Abstract Nitrene transfer (NT) is a convenient strategy to directly transform C–H bonds into more valuable C–N bonds and exciting advances have been made to improve selectivity. Our work in silver-based NT has shown the unique ability of this metal to enable tunable chemosite-, and stereoselective reactions using simple N-dentate ligand scaffolds. Manipulation of the coordination environment and noncovalent interactions around the silver center furnish unprecedented catalyst control in selective NT and provide insights for further improvements in the field.

- 1 Introduction
- 1.1 Strategies for Nitrene Transfer
- 1.2 Brief Summary of Chemocatalyzed Nitrene Transfer
- 1.3 Focus of this Account
- 2 Challenges in Chemocatalyzed Nitrene Transfer
- 2.1 Reactivity Challenges
- 2.2 Selectivity Challenges
- 2.3 Chemoselective Nitrene Transfer
- 2.4 Site-Selective Nitrene Transfer
- 2.5 Enantioselective Nitrene Transfer
- 3 Summary and Perspective
- 3.1 Future Opportunities and Challenges
- 3.2 Conclusion

Key words silver, nitrene transfer, C–H functionalization, amination, amines, asymmetric

1 Introduction

1.1 Strategies for Nitrene Transfer

The presence and importance of nitrogen in natural products, bioactive molecules, pharmaceuticals, polymers, and catalyst ligands has stimulated the development of a diverse array of methods to introduce C–N bonds into readily available starting materials. One common strategy is ni-

trene transfer (NT), which involves the addition of a reactive, electron-deficient nitrogen species, typically supported by a transition metal, to an alkene (aziridination) or into a C–H bond (C–H amination). This class of reactions has been of intense interest in recent years, given that the ability to transform C–H bonds directly into new C–N bonds can streamline the syntheses of many useful compounds and synthetic building blocks.¹ From an academic perspective, the diversity of transition metals that support reactive nitrene species makes the study of NT a rich opportunity to better understand the fundamental details of how electronic structure impacts reactivity and selectivity.

Current strategies for NT can be divided into two main approaches: biocatalysis and chemocatalysis. The former takes advantage of Nature's efforts over millions of years to evolve enzymes that are capable of selectively oxidizing a specific C-H bond from amongst many candidates. Several research groups, most notably the Arnold group, have developed ways to speed up this evolutionary process to develop enzymes that catalyze C-H functionalization reactions that do not regularly occur in nature, including the direct amination of C-H bonds.² Despite the high selectivities and turnover numbers associated with biocatalysis, not all laboratories have the infrastructure or expertise to carry out directed evolution. Substrate scope can also be limited, due to the need to utilize solvent systems compatible with enzymes. Additionally, enzymes are often co-factor dependent and may be inactivated by higher temperatures, extreme pH value, high salt concentrations, and polar organic solvents.3

While biocatalysis is an excellent choice for optimizing manufacturing routes to commercial drugs and agrochemicals, the early-stage exploration and late-stage functionalization of complex molecules benefit from chemocatalyzed NT. Several broadly accessible and highly modular catalyst systems have been developed to enable expedient reaction

[♦] Indicates equal authorship.

screening; in fact, over ten different transition metals are known to promote NT reactions, with Rh, Ru, Ir, Fe, Mn, Co, Cu, and Ag among the more extensively researched.⁴ NT reactions are surprisingly robust, despite the intermediacy of a highly reactive nitrene species, and are often insensitive to atmospheric air and water. Key highlights of the NT field are presented in Section 1.2; however, very few strategies in the literature deviate from the use of substrate control to influence the outcome of the C–N bond formation. This Account focuses on the unique features of silver-catalyzed NT that make it useful for tuning the chemo-, regio-, site-, and enantioselectivity of NT processes in ways that other metals have been unable to do thus far.

1.2 Brief Summary of Chemocatalyzed Nitrene Transfer

The chemistry of metallonitrenes has a long history, going back to Kwart and Khan's first description of the copper-catalyzed decomposition of benzosulfonyl azides in

1967.⁵ In that report, Kwart and Kahn proposed the intermediacy of a copper–nitrene species capable of promoting either an alkene aziridination or a C–H insertion process. However, it was not until several years later that Breslow employed catalytic Mn(III)(TPP) (tetraphenyl-porphyrin, TPP), Fe(III)(TPP), and Rh₂(OAc)₄, in combination with an iminoiodinane nitrogen source, to promote intramolecular C–H amidation. Importantly, this work led to a model system for analogous transformations of C–H to C–O bonds performed by the cytochrome P-450 class of enzymes.⁶ In the early 1990's, Evans⁷ and Jacobsen⁸ expanded on Breslow's initial findings and reported a series of Cu catalysts, supported by bis(oxazoline) (BOX) and salen-type ligands, to promote asymmetric aziridination, albeit with limited scope.

Over the past 20 years, the development of improved NT catalysts has continued unabated. For example, Breslow's initial reports inspired the design of more efficient dinuclear Rh(II) catalysts. Beginning in early 2000's, Du Bois reported a series of Rh_2L_n complexes supported by carboxyl-

Biographical Sketches



Logan E. Vine grew up in Sparks, Nevada and earned his undergraduate degree in chemistry from Willamette University in 2017. There he performed analytical chemistry research on distributions of estrogen and

estrogen derivatives throughout the wastewater treatment process for Prof. David Griffith. He started his graduate studies at University of Wisconsin Madison under the leadership of Prof. Jennifer Schomaker. His research has focused on Ag-catalyzed inter- and intramolecular nitrene transfer, as well as the functionalization of allenes using palladium chemistry.



Emily E. Zerull graduated from Calvin University with a BS in chemistry, where she researched under Prof. Carolyn Anderson. She then entered the

PhD program at University of Wisconsin-Madison, where she is currently undertaking her graduate studies under the direction of Prof. Jennifer Schomaker. Her work focuses on the development of Ag-catalyzed asymmetric nitrene transfer reactions through rational catalyst and ligand design.



Jennifer M. Schomaker received her PhD in 2006 from Michigan State University, working with Prof. Babak Borhan. After completing an NIH postdoctoral fellowship at UC-

Berkeley under Prof. Robert Bergman and Prof. F. Dean Toste, she began her independent career at the University of Wisconsin-Madison in 2009. Her research interests include catalyst-controlled C–H oxidations, new methods for the syntheses of new *N*-heterocycle chemical space, and the total synthesis of complex bioactive molecules.

Figure 1 (A) Selection of common transition-metal catalysts for NT. (B) Examples of the diverse geometries of silver(I) NT catalysts.

ate bridging ligands that achieved efficient NT with excellent functional group tolerance. Du Bois' $Rh_2(esp)_2$ (Figure 1A, $\alpha,\alpha,\alpha',\alpha'$ -tetramethyl-1,3-benzenedipropionic acid, $esp)^{9c}$ catalyst is particularly powerful for intra- and intermolecular NT and displays excellent utility for the late-stage functionalization of complex molecules. 9h

The Dauban group has described the use of chiral sulfonimidamide nitrene precursors with Rh catalysts to achieve diastereoselective intermolecular C-H amidation.¹⁰ Ru catalysts supported by salen, porphyrin, and bridging 2hydroxypyridine ligands have also been reported, some of which are capable of enantioselective aziridinations of terminal and simple alkenes.8 NT catalysts based on the firstrow transition metals Co, Fe and Mn are typically supported by ligands that include modified porphyrins, phthalocyanines, and other porphyrin mimics,¹¹ while Cu is utilized with a wide variety of supporting ligands such as bis(oxazolines), diimines, and scorpionates. 12 Of particular note are Co catalysts developed by Zhang, which include several asymmetric versions with chiral extensions of the porphyrin scaffold (Figure 1, A) to enable enantioselective NT.13 More recently, the Chang group described a series of Ir catalysts that harness noncovalent interactions to direct both racemic and enantioselective syntheses of γ -lactams from dioxazolones. This innovative strategy circumvents the detrimental Curtius rearrangement that typically precludes the use of amide derivatives as suitable nitrene precursors.14

The first example of silver-catalyzed NT was reported by the He group in 2003.¹⁵ AgNO₃ supported by a 4,4′,4″,-tri-tert-butyl-2,2′:6′,2″-terpyridine (*t*-Bu₃tpy) ligand was proposed to form a dinuclear silver(I) complex that catalyzed intermolecular alkene aziridination (Figure 1, B). A later

publication from the same group employed a silver catalyst supported by bathophenanthroline to achieve intramolecular amidations of tertiary and benzylic C–H bonds. In 2013, Pérez reported sulfonimidamide nitrene precursors and Ag(I) supported by trispyrazolylborate (Tp) scorpionate ligands for intermolecular amidations of benzylic and alkyl C–H bonds. Pérez later published a mechanistic study investigating this catalyst scaffold in aziridination; the long-assumed concerted mechanism was deemed unlikely, due to a computationally predicted lower energy pathway involving a triplet silver nitrene intermediate. More recently, the Bach group designed an asymmetric NT method that relies on hydrogen-bonding interactions between a chiral phenanthroline-based silver catalyst and a pyridone directing group built into the substrate.

1.3 Focus of this Account

This Account describes the design principles underlying our group's development of silver catalysts capable of tunable and selective NT; a general catalytic cycle is illustrated in Figure 2A. Traditionally, silver salts and their complexes are used as oxidants, halide scavengers, additives, or heterogeneous catalysts; thus, we were intrigued by He's report that two AgOTf supported by two *t*-Butpy ligands forms a dimer that efficiently catalyzes NT.¹⁵ Two unique features of silver coordination complexes stand out when compared to typical NT catalysts: the diversity of simple Ndentate ligands able to support Ag(I) complexes and their dynamic behavior in solution. We hypothesized an ability to manipulate this dynamic behavior to our advantage could furnish new and tunable catalysts to tackle difficult selectivity challenges in NT using a single metal (Figure 2B).



Figure 2 (A) General catalytic cycle for NT. (B) Selectivity challenges in NT.

In particular, we were interested in catalysts able to tune the chemoselectivity of intra- and intermolecular NT, as well as the site selectivity between two C–H bonds in either different or similar steric and electronic environments.

This Account describes our efforts to leverage the versatility of silver to selectively distinguish between C-H bonds with similar bond-dissociation energies (BDE) and/or steric environments, even overriding inherent substrate preferences to favor a less reactive site. Recent efforts in asymmetric Ag-catalyzed NT are presented; excitingly, we have made significant inroads into the development of general, modular catalysts for asymmetric aziridination and C-H bond amidation. The Account concludes by highlighting future opportunities and challenges still remaining in the field.

2 Challenges in Chemocatalyzed Nitrene Transfer

2.1 Reactivity Challenges

The relative strength of the C–H bond, compared to other common functional groups, renders it inert to many traditional organic transformations. While extensive research over the past decade has yielded several strategies for C–H bond functionalization, NT remains one of the most efficient methods to directly transform unactivated C–H bonds into new C–N bonds. NT employs a neutral, six-electron nitrogen species (nitrene) that can exist in either a singlet (where the four valence electrons are paired) or triplet (where there are two unpaired electrons) form. Free nitrenes are generated via thermolysis or photolysis of various precursors, typically azides;²⁰ however, the extreme reactivity of the free nitrene, coupled with the harsh conditions under which these species are generated, often lead to poorly selective reactions and mixtures of products.

The generation of metal-supported nitrenes offers an attractive alternative method to generate electron-deficient nitrenes for C-H functionalization. Along with more controlled reactivity, these species are generated from accessible nitrogen precursors such as carbamates, sulfamates, and sulfonamides. The precursor is treated with a hypervalent iodine oxidant to generate an intermediate imidoiodinane,

which is transferred to the metal to form the reactive amidating species (see Figure 2A). Pre-oxidized nitrenes have also been exploited to generate the metal nitrene species without the need for a hypervalent iodine oxidant.²¹ While metal-stabilized nitrenes have been successfully used to limit side reactions and decomposition pathways, the amidation of strong secondary and primary aliphatic C–H bonds sites remain challenging, spurring investigations into more reactive metal nitrene species.

2.2 Selectivity Challenges

In addition to meeting the reactivity challenge for C–H bond amidation, achieving predictable control over selectivity with broad substrate scope remains the predominant challenge in NT. While certain types of selectivity can be accomplished using particular catalyst–substrate combinations, the use of one metal to achieve tunable NT by altering the ligand is rare, especially when it is desirable to override substrate control.

An exciting opportunity in NT involves identifying strategies to achieve the ultimate goal of tunable catalyst control over chemo-, site-, and stereoselectivity when multiple potential reactive sites are present. Typically, site selectivity is accomplished through substrate control, where potential C–H bonds are differentiated in terms of their reactivity. For example, benzylic C-H bonds activated by hyperconjugation with the adjacent π -system have been selectively amidated using several metals, ligands, and precursors. However, inconvenient nitrene sources are often required, depending on whether β - or γ -intramolecular amidation products are desired, resulting in extra or low-yielding steps. Catalyst-controlled NT, where the metal and its supporting ligands bear primary responsibility for dictating the specific site of amidation, is a far more versatile strategy, in that it permits flexible installation of new C-N bonds at diverse C-H bonds in a readily tunable manner. With these powerful new tools, simple hydrocarbons and complex molecules alike can be readily upgraded to more valuable building blocks and drug candidates.

Many factors influence the outcome of NT in a given C–H amidation event (Figure 3). Catalyst features include the metal, the steric or electronic features of the ligands, the counteranion, and the metal-to-ligand ratio. Substrate pa-

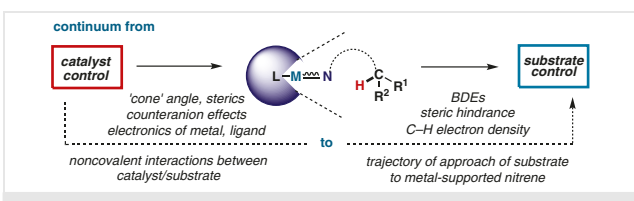
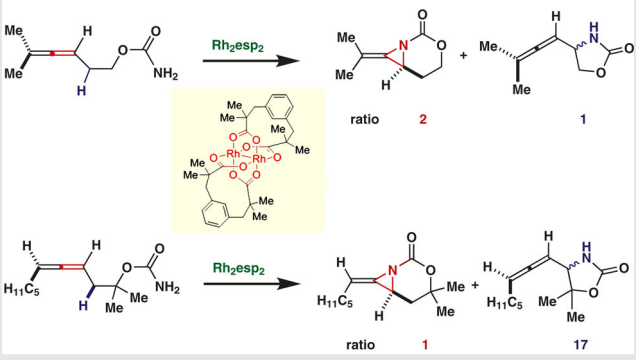


Figure 3 Spectrum from catalyst control to substrate control for transition-metal-catalyzed NT

2.3 Chemoselective Nitrene Transfer

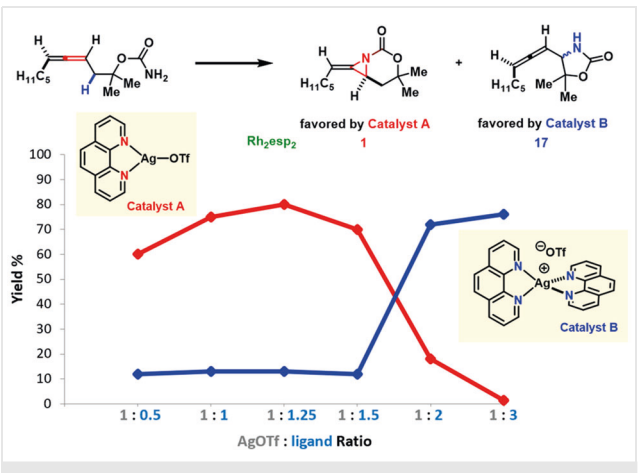
2.3.1 Intramolecular Chemoselective Nitrene Transfer

Our foray into silver-catalyzed NT arose from difficulties encountered in identifying methods to oxidatively transform allenes into densely functionalized and stereochemically rich amine triads.²² Chemoselective aziridination of homoallenic carbamate precursors was key to the successful, rapid elaboration of these axially chiral precursors into amine building blocks. Unfortunately, despite significant effort, a Rh catalyst capable of furnishing predictable chemoselectivity with broad substrate scope could not be identified. The ratio of aziridination/C–H amidation products varied wildly, depending on the allene substitution pattern (Scheme 1). Other popular catalysts based on Cu, Ru, Fe, and Mn also failed to provide satisfactory results.



Scheme 1 Substrate-based variations in selectivity for aziridination versus C–H amidation using Rh₂esp₂

Inspired by He's report of Ag(I) as an efficient catalyst for NT¹⁵ and the rich diversity of coordination geometries available to Ag(I) complexes supported by a variety of nitrogenated ligands,²³ the experiments shown in Scheme 2 were carried out.²⁴ We were curious if changes to the Ag-OTf/1,10-phenanthroline (phen) ratio would furnish two different potential catalytic species that could alter the chemoselectivity of the NT.



Scheme 2 Product distribution of Ag-catalyzed NT with varied AgOTf/phenanthroline ratio

Indeed, low loadings of phen displayed a preference for aziridination, providing significantly higher yields of the desired methyleneaziridine as compared to Rh₂esp₂. Decreasing the ratio of AgOTf/phen by increasing the amount of phen suppressed aziridination and gave excellent selectivity for C–H insertion. This chemistry showed broad scope for both homoallenic and homoallylic carbamates, enabling NT to be toggled between aziridination and C–H amidation by a simple change in the Ag/ligand ratio.

2.3.2 Understanding the Reasons for Chemoselectivity

The divergent chemoselectivity in Scheme 2 was ascribed to the influence of the different coordination environments around the silver center on the trajectory of approach of the functional group (alkene or C–H bond) to the putative silver nitrene. Unfortunately, direct support of this hypothesis was not possible, due to the transient nature of metal nitrenes. Attempts to determine how the Ag/ligand ratio influences the equilibrium of the catalyst resting states were complicated by the dynamic behavior of these complexes in solution, even at –80 °C (Figure 4). Despite this dynamic behavior, NMR studies show a clear shift in the predominant silver species with increased ligand loading. Combined with pulse gradient spin echo and MALDI-MS experiments, these studies show a shift in the major

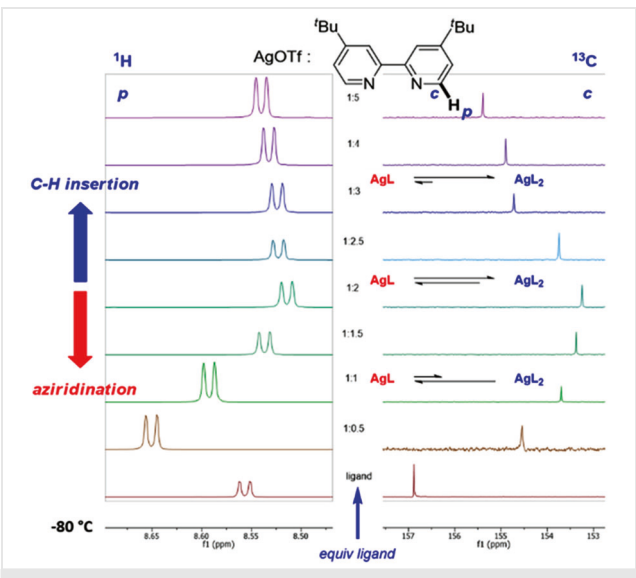


Figure 4 VT-NMR studies showing change in chemical shift with increased *t*-BuBipy loading

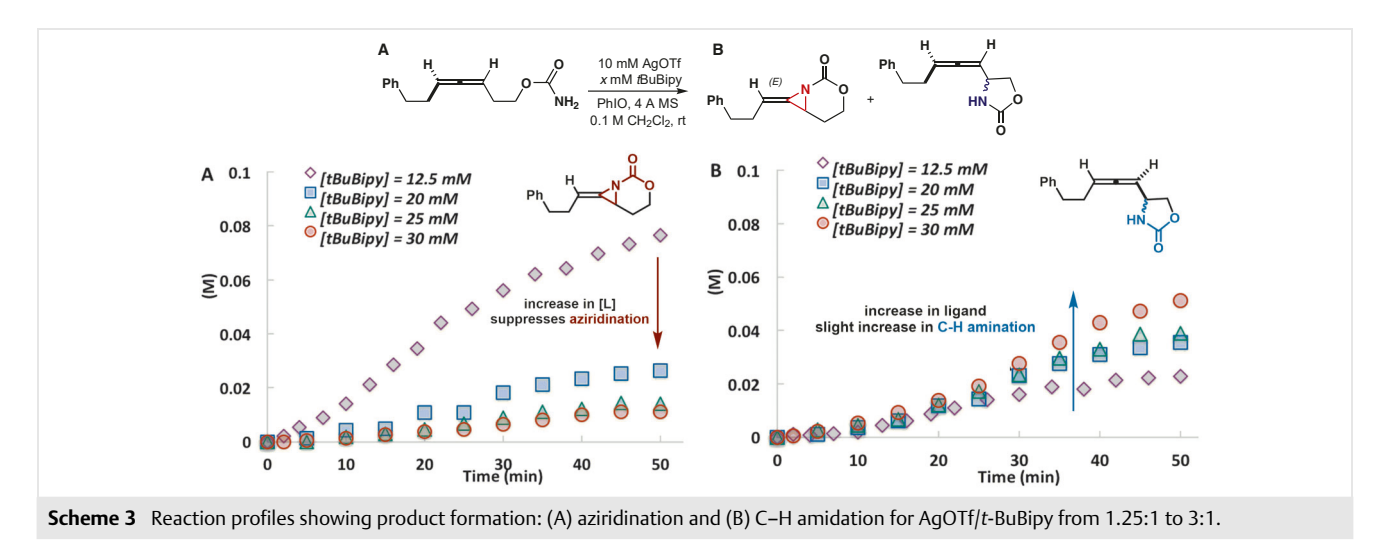
Typical mechanistic probes of reactivity (kinetic isotope effect studies, stereochemical retention, radical clock experiments) all indicated that the Ag/ligand ratio did not alter the mechanism of the intramolecular NT reaction.²⁵ Tracking rates of aziridination vs. C–H amidation at varying ratios of AgOTf/t-BuBipy with the same AgOTf and substrate concentration revealed aziridination is suppressed at high ligand loadings (Scheme 3A). In contrast, the AgOTf/t-BuBipy ratio has a minimal impact on the rate of the C–H amidation, particularly in the early stages of the reaction (Scheme 3B). Thus, we concluded that tunable chemoselectivity largely results from steric effects that suppress azirid-

ination at high ligand loadings, while leading to only a slight increase in the rates of C–H amidation.

2.3.3 Intermolecular Chemoselective Nitrene Transfer

Tunable, intermolecular chemoselectivity in silver-catalyzed NT proved challenging. Altering the AgOTf/ligand ratio did not provide general and predictable changes to the chemoselectivity, perhaps due to the dynamic nature of the catalyst and the increase in potential trajectories for approach of the substrate to the metal-supported nitrene. Nonetheless, the diversity in the coordination geometries of silver(I) complexes for NT provided a solution, albeit one limited to tunable amidations of cyclic alkenes. The dimeric complex formed from t-Bu₃tpy ligands and AgOTf, as seen in both the solid (single-crystal X-ray structure) and solution (DOSY NMR) states, in combination with hexafluoroisopropan-2-yl sulfamate (HfsNH₂) as the nitrene precursor, furnished selective aziridination of substituted cyclohexenes.²⁶ In contrast, AgOTf supported by a tris(2pyridylmethyl)amine (tpa) ligand, using 2,6-difluorophenyl sulfamate (DfsNH₂) as the nitrene precursor, preferred amidation of the allylic C-H bond.

To shed insight into the reasons for this tunable intermolecular NT, computations were carried out on the optimized nitrene species resulting from the reaction of each catalyst with imidoiodinane formed from NfsNH $_2$ (Scheme 4B and 4C). In the dimeric silver complex supported by t-Bu $_3$ tpy (Scheme 4B), one of the two OTf counteranions is dissociated from the metal center, leaving two inequivalent Ag sites. The Ag bound to the nitrene (AgN) is otherwise bound only to the N atoms of the t-Bu $_3$ tpy ligands, having displaced the counteranion from the coordination sphere; the other silver (AgO) is coordinated to the pyridines of the ligand and a triflate anion. Computations on the nitrene intermediate supported by (tpa)AgOTf shows the nitrogen is bound in the equatorial site, cis to the tertiary amine of the



Scheme 4 (A) Product distributions for tunable intermolecular NT under different conditions. (B) Optimized structure for aziridination catalyst. (C) Optimized structure for C–H amidation catalyst.

ligand, while the triflate is bound in the axial site (Scheme 4C). Thus, tunable chemoselectivity appears to arise from differences in the steric profiles of the Ag–nitrene intermediates.

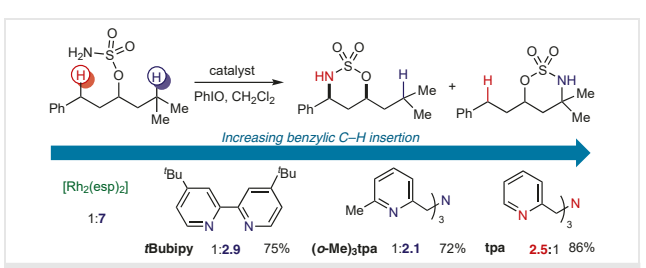
Furthermore, two distinct NT mechanisms were observed in computational studies of chemoselective, intermolecular NT. Both catalysts were found to proceed through a triplet-state intermediate Ag(II) species, coupled to a nitrogen radical anion. At this point, the catalyst depicted in Scheme 4B proceeds through a very late transition state for the initial hydrogen atom transfer (HAT), followed by a barrierless radical recombination step to preserve the stereochemical information in both cyclic and acyclic alkene substrates. In contrast, the catalyst supported by tpa (Scheme 4C) was computed to have an early transition state, yielding a discrete radical intermediate in the HAT step that erodes stereochemical information and responds to the addition of a radical inhibitor. These computations are supported by a number of experimental mechanistic studies. The major distinction between these two mechanisms appears to be the extent to which the Ag-N bond breaks during the HAT transition state; more extensive Ag-N bond cleavage in the transition state results in a reduced lifetime of the radical intermediate, leading to experimental observation of an essentially 'barrierless' radical recombination.

Future work is directed towards improving the scope of the chemoselective NT by tuning the steric environment around the putative silver nitrene by altering the ligand, nitrene precursor or counteranion identity in a manner that minimizes the impact on the electronic structure.

2.4 Site-Selective Nitrene Transfer

2.4.1 Choosing between Different C–H Bonds

Having addressed issues of tunable chemoselective NT using silver catalysis, we next turned our attention to designing catalysts for tunable, site-selective C-H amidation. The intramolecular competition between two different types of C-H bonds (Scheme 5) was examined in the form of a weak benzylic C-H bond (BDE ca. 90 kcal/mol) and a more electron-rich 3° alkyl C(sp³)-H bond (BDE ca. 97 kcal/mol).²⁷ Interestingly, a significant variation in site selectivity was noted using different ligands with AgOTf. Similar selectivities were noted with Rh_2esp_2 and $Ag(t-Butpy)_2$, with both catalysts favoring amidation at the tertiary site. In contrast, use of the tetradentate tris(2-pyridylmethyl)amine (tpa) ligand reversed the selectivity in favor of amidation of the benzylic C-H bond. The observation that a (o-Me)₃tpa ligand restored the preference for amidation of the tertiary C-H bond suggested that a change in the coordination geometry of the various catalysts might be influencing the site selectivity of the NT event.28

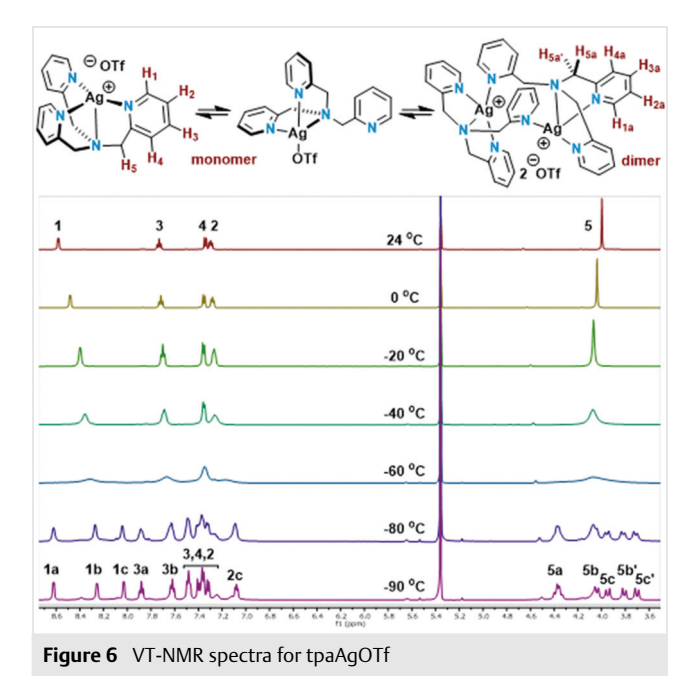


Scheme 5 Comparison of catalysts for site-selective insertion into different types of C–H bonds

Variable temperature (VT) NMR studies of (o-Me)₃tpaAgOTf (Figure 5) and tpaAgOTf (Figure 6) were carried out to gain insight into how the fluxional behavior of these two complexes might play a role in influencing the site selectivity of C–H amidation. In (o-Me)₃tpaAgOTf, the solid-state structure is a dicationic dimer with a five-coordinate geometry at each of the two silver atoms; however, further investigation painted a very different picture of its solution-state behavior. In solution, there are two fluxional processes that may influence the site selectivity of NT: the equilibrium between monomeric and dimeric structures, and the rapid exchange of ligands on and off the metal center.²⁹

From +24 °C to -20 °C, the ¹H NMR spectra show a single set of resonances for the CH_2 and CH_3 protons, indicative of a monomeric complex with rapid exchange of the pyridine arm(s) of the ligand. The broadening of the monomer peaks at lower temperatures are further evidence of interconversion between two N-tridentate forms through the intermediacy of a N-tetradentate complex. At -40 °C, the three singlets in a 1:1:1 ratio at δ = 2.50, 2.27, and 2.16 ppm arise from a dimeric species. At -90 °C, the silver complex is

Figure 5 VT-NMR spectra for (o-Me)₃tpaAgOTf



found residing largely in this dimeric form. DOSY-NMR studies of $(o\text{-Me})_3$ tpaAgOTf in CD₂Cl₂ at 25 °C, -20 °C, and -90 °C showed monomer/dimer ratios of 90:10, 56:44, and 22:78, respectively.

The DOSY-NMR of tpaAgOTf in CD_2Cl_2 at 25 °C, -20 °C, and -90 °C showed monomer/dimer ratios of 60:40, 55:45, and 19:81, respectively. At low temperatures, distinct aryl protons for the magnetically distinct pyridine rings are seen. The individual proton signals begin to coalescence as the temperature increases, indicating either a preference for monomer > dimer or rapid exchange of the pyridine arms of monomeric complex on the NMR time scale.

The challenge of establishing design principles for fluxional catalysts stimulated our efforts to minimize dynamic behavior. To this end, the sp³ nitrogen of the tpa was 'pinned back' in a piperidine ring and a Me group added to the remaining arm. Complexation of the new ligand with AgOTf gave monomeric $[(\alpha-Me)-anti-Py_3Pip]$ AgOTf, which displayed limited fluxional behavior (Figure 7).30 At low temperatures, the three protons α to the pyridine ligand 'arms' all exhibit distinct signals in the ¹H NMR spectra. The equatorial $H_{1'}$ shows small, unresolved $J_{eq/eq}$ and $J_{eq/eq}$ couplings in the broad singlet. The axial H₁ proton shows a large $J_{ax,ax}$ coupling, although the small $J_{ax,eq}$ is not resolved; H₂ is a broad quartet. No evidence of dimer formation is seen throughout the entire temperature range of the VT-NMR experiment; however, peak broadening near room temperature is indicative of rapid exchange of the pyridine arms on the piperidine ring.

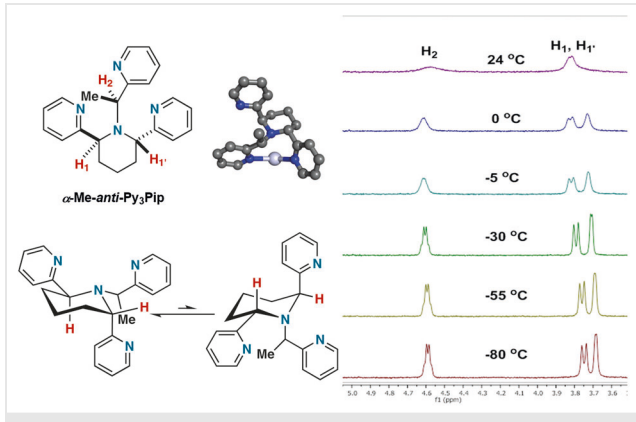


Figure 7 VT-NMR spectra showing the limited fluctional behavior of $[(\alpha-Me)-anti-Py_3Pip]AgOTf$

With this less dynamic system in hand, the temperature and the solvent were further optimized to improve the selectivity for benzylic C–H amidation to 8.5:1 (Scheme 6A). Application of these changes to the original tpaAgOTf also gave improved selectivity. However, while decreased fluxionality was demonstrated to be beneficial, the reasons why benzylic C–H bond amidation was preferred over the tertiary alkyl C–H bond required further investigation.

Computations of the lowest-energy triplet states of Ag nitrenes supported by excess *t*-Bubipy and tpa, ligands that yield opposite site selectivity (Scheme 6B), indicate that both Ag-nitrene reactant complexes are best described as

Scheme 6 (A) Optimization of improved catalyst for benzylic C–H bond insertion. (B) Computed transition states showing evidence of noncovalent interactions as the origin of benzylic reactivity.

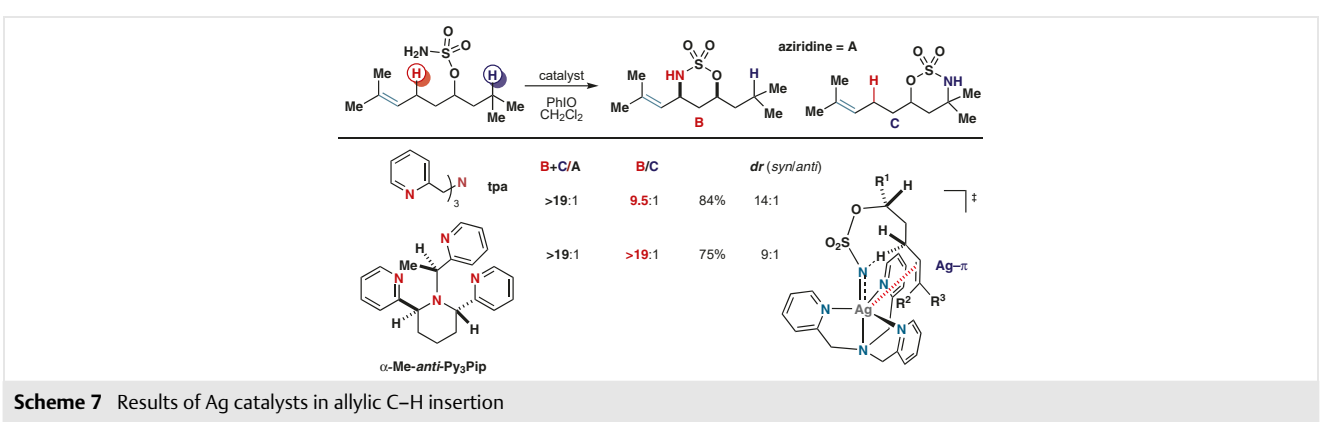
Ag(II)–nitrene radical anions. Critical points along the triplet potential surfaces were scanned for both complexes, and the transition states (TS) for either benzylic or 3° C–H amidation were located. Importantly, substrate–aryl···tpa–pyridyl π ··· π interactions between 3.22–3.34 Å were present in the nitrene supported by the tpa ligand, while no such π ··· π interactions were present in any pro-3° structures. In contrast, the silver nitrene supported by the t-Bubipy ligand is too sterically congested to enable effective π ··· π interactions between the ligand and the substrate. These observations led us to propose that aryl–aryl noncovalent interactions were likely responsible for the switch in site-selective C–H amidation.

Substrates with allylic C–H bonds present the possibility of competing aziridination (Scheme 7). As high ligand/Ag ratios disfavor aziridination, we proposed ligands enforcing tridentate or higher-coordinated Ag complexes might favor C–H amidation, with a preference for allylic C–H bond over other reactive bonds, including alkenes and 3° alkyl $C(sp^3)$ –H bonds. Indeed, the use of either (tpa)AgOTf or [(α -Me)-

anti-Py₃Pip]AgOTf in CHCl₃ at -20 °C delivered excellent chemoselectivity, favoring C-H amidation over aziridination by a >19:1 ratio. The site selectivity was also good, with a marked preference for amidation of the allylic over the tertiary alkyl. The reasons for site-selective allylic C-H amidation were traced to Ag- π interactions in the transition state. Computational studies similar to those employed for probing π - π interactions (Scheme 7) showed an Ag- π interaction at 3.60 Å in the transition state of a nitrene derived from (tpa)AgOTf. Computations also predicted a preference for the *syn* diastereomer, matching the experimental results.

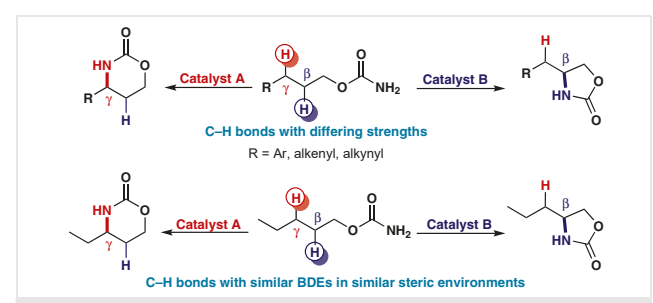
Poor selectivity in the amidation of propargylic over electron-rich 3° alkyl $C(sp^3)$ –H bonds was noted using previously reported catalysts. We hypothesized selective amidation at the propargylic C–H bond to furnish valuable propargylamine building blocks could be improved using two different design strategies. In the first, increasing the steric bulk around the silver center might bias approach of a less sterically demanding propargylic C–H bond to the putative silver nitrene. In contrast, minimizing steric pressure at the metal could enable a directing silver– π noncovalent interaction with a positive impact on the site selectivity.

(t-Bubipy)₂AgOTf resulted in poor selectivity for propargylic C-H amidation, as the high coordination at the metal center may inhibit potential π -Ag interactions. A less congested tpaAgOTf complex delivered the propargylamine as the major product, albeit in low selectivity. The $[(\alpha-Me)$ anti-Py₃Pip]AgOTf catalyst, which displayed good selectivity for benzylic C-H amidation (Scheme 8A),32 was promising, although steric repulsion in the orientation required for an effective Ag- π interaction suggested that control over the trajectory of approach of the substrate to the metal nitrene might be more effective. Fortunately, a dimeric complex resulting from complexation of AgOTf to a 2,6-bis[1,1bis(2-pyridyl)ethyl]pyridine (Py₅Me₂) ligand appeared to provide a sufficiently hindered pocket around the Ag nitrene, such that amidation is reduced at the bulkier tertiary site. Improved propargylic C-H amidation using [(Py5Me2)AgOTf]2 was consistent across a broad scope of alkynes (Scheme 8B).



Scheme 8 (A) Comparison of catalysts for selective propargylic C-H insertion. (B) Examples of improved selectivity using a bulky [(Py₅Me₂)AgOTf]₂ catalyst.

Overall, these combined studies resulted in the ability to selectively tune for benzylic, allylic, or propargylic C-H bonds over tertiary bonds (and vice versa) using the same metal and provided key design principles to predictably manipulate the reactivities of silver catalysts based on steric effects and noncovalent interactions.



Scheme 9 Site-selectivity challenges for C–H bonds with inherent substrate preference (top) or similar steric and electronic properties (bottom)

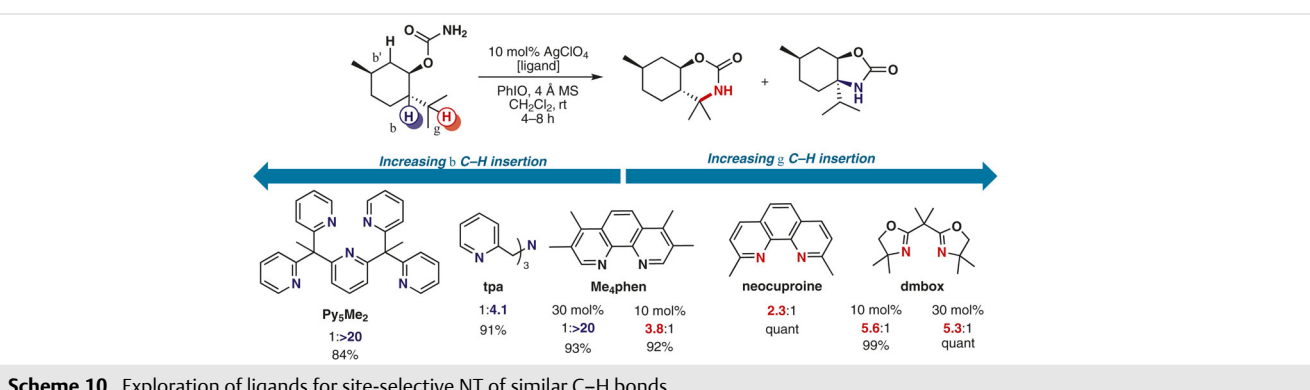
2.4.2 Choosing between Similar C-H Bonds

Two challenges in chemocatalyzed NT that remain largely unmet are the ability to override the preference for amidation of an 'activated' C-H bond, such as an allylic, propargylic, or benzylic site, in favor of an unactivated methylene C-H bond (Scheme 9) and the ability to predictably choose between two C-H bonds that reside in similar steric environments and/or have similar BDEs. We postulate this selectivity is hard to achieve with typical NT catalysts due to an inability to significantly alter the ligand scaffold in a manner that allows for predictable control over the trajectory of approach of the targeted C-H bond to the putative metal nitrene. However, the flexibility in coordination environments displayed by Ag(I) catalysts suggested that judicious ligand choice might permit tuning of the trajectory of approach of the C-H bond to the nitrene intermediate and manipulation of the site selectivity of the NT.

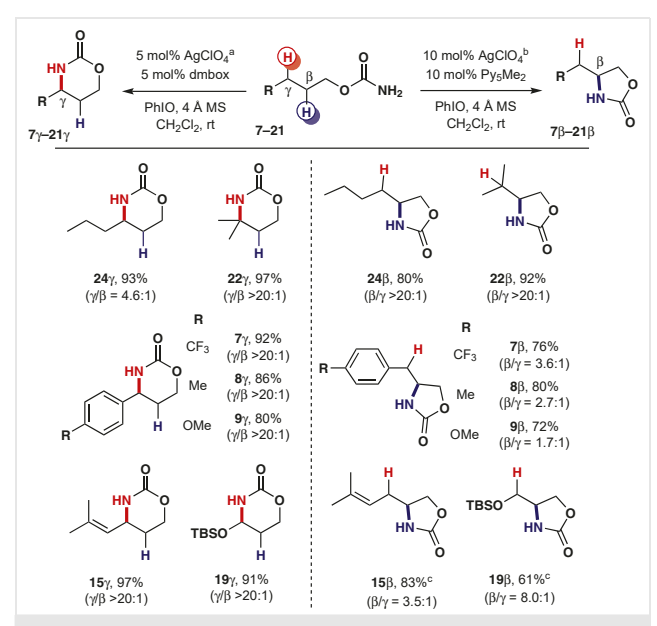
The carbamate ester of menthol contains two competing 3° alkyl C(sp³)-H bonds at carbons β and γ to the carbamate oxygen, making it an excellent candidate to test true catalyst control. Initial investigations into high coordinate ligands for Ag-catalyzed NT, including tpa, gave a strong preference for amidation at the β site (Scheme 10).³³

Interestingly, changing the ligand/metal ratio of Me₄phen from 2:1 to 1:1 reversed the site selectivity from β to γ , just as it reversed chemoselectivity in previous studies with similar ligands. This led us to explore other bidentate N-donors in 1:1 ligand/metal ratios, including neocuproine and a dimethyl-substituted bis(oxazoline) ligand, dmbox. Both catalysts preferred γ amidation, with dmbox giving the highest reactivity/selectivity and near-quantitative yield. Gratifyingly, the sterically hindered [(Py₅Me₂)Ag-ClO₄]₂ catalyst previously designed in our group resulted in complete selectivity for the β -site.

Monomeric (dmbox)AgClO₄ and dimeric [(Py₅Me₂)Ag- $ClO_4]_2$ were chosen for further study due to their excellent selectivity and reactivity. A selection of substrates is illustrated in Scheme 11, highlighting the unique ability of silver to tune the intramolecular amidation of a β or γ C-H bond by a



Scheme 10 Exploration of ligands for site-selective NT of similar C-H bonds



Scheme 11 Selected examples of tunable NT enabled by Ag-catalysts. a γ-C-H amidation: AgClO₄/dmbox (10 mol%), PhIO (2.0 equiv), 4 Å MS, rt, 0.05 M CH₂Cl₂, 4–12 h. b β-C-H amidation: AgClO₄/Py₅Me₂ (10 mol%), PhIO (2.0 equiv), 4 Å MS, rt, 0.05 M CH₂Cl₂, 2–12 h. c β-C-H amidation: AgClO₄/Py₅Me₂ (5 mol%), PhIO (2.0 equiv), 4 Å MS, rt, 0.05 M CH₂Cl₂, 2–12 h.

The remarkable selectivity that enabled tuning between similar C–H sites inspired us to assess whether these catalysts could override inherent reactivity to achieve selective amidation at less reactive C–H bonds. Historically, in the presence of a significant electronic driving force, such as a 3° C–H bond, a less activated 2° aliphatic site will show poor reactivity, regardless of the substrate or catalyst employed. Interestingly, $[(Py_5Me_2)AgClO_4]_2$ was able to overcome this limitation and amidate stronger 2° aliphatic C–H bonds (BDE >90 kcal/mol) over weaker, activated benzylic, allylic, and ethereal C–H bonds (BDE ~80-85 kcal/mol). Notably, even electron rich aryls did not switch the preference back to the activated γ C–H bond.

Mechanistic studies revealed similar KIE values and retention of stereochemistry with both (dmbox)AgClO₄ and [(Py₅Me₂)AgClO₄]₂, suggesting both proceed via a mechanism involving hydrogen-atom transfer, followed by rapid radical rebound, as previously discussed for other Ag-catalyzed NT systems. Application of Charton's modified Taft equation and steric parameters to the data gave a linear

free-energy relationship (LFER) that correlates steric environments of both the substrate and ligand to the site-selectivity of the NT event.

Thus, steric differences are the most likely reason for the divergent site-selective amidation. Computations show a strong preference for a near-linear HAT transition state (TS), favoring a seven-membered TS in the absence of external steric effects in the relatively open (dmbox)AgClO₄ (Figure 8). However, the cagelike structure of $[(Py_5Me_2)AgClO_4]_2$ creates a relatively small pocket that favors a six-membered TS to drive reactivity towards amidation at the β -site.

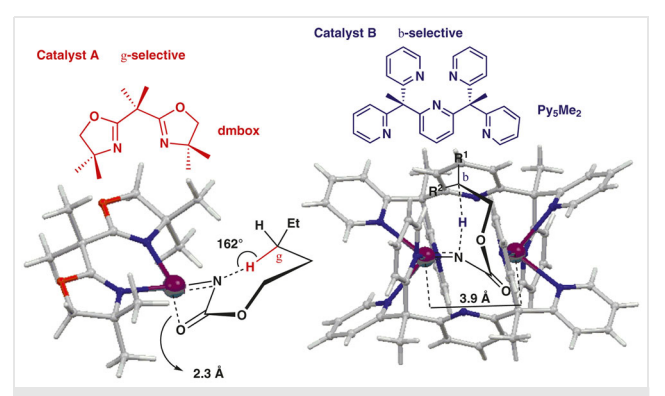


Figure 8 Selectivity model based on computed structure of (dm-box)AgClO₄ (left) and the single crystal X-ray structure of $[(Py_5Me_2)Ag-ClO_4]_2$ (right)

2.4.3 Late-Stage Functionalizations Using Silver-Catalyzed Nitrene Transfer

The hydrogen-bonding capabilities of amines are known to interact with binding pockets in biological systems. Thus, a compelling reason for the continued development of chemocatalysts for NT is their potential for tunable late-stage functionalization of natural products, pharmaceuticals, and readily available commercial building blocks. We have demonstrated that our methodologies are compatible with complex molecules of biological relevance and thus have high values for derivatization and analogue synthesis (Scheme 12).³³

Among tested molecules are nonsteroidal anti-inflammatory drugs oxaprozin and nabumetone as well as essential omega-6 fatty acid linoleic acid that can be subsequently ring opened into the corresponding amino alcohols.

2.5 Enantioselective Nitrene Transfer

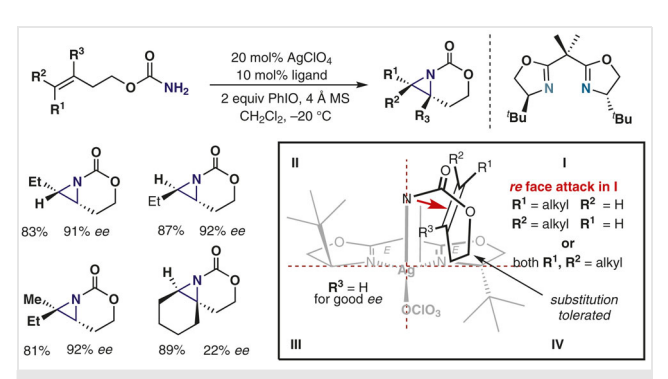
Enantioselective, chemocatalyzed NT has been a long-standing challenge in the field. While there are reports of success using various catalysts, including Rh, Co, Ru, Ir, and Cu, large gaps in the types of substrates and products available remain. The design of modular catalysts based on a single metal remains elusive, but would provide a desirable pathway towards expanding the utility of asymmetric NT.

Scheme 12 Late-stage functionalization utilizing Ag-catalyzed NT. a Ring-opening of C–H amidation product was carried out; 0.2 M in 1,3-diaminopropane, reflux. AgClO₄/Py₅Me₂ (10 mol%). Selectivity determined at the Ag-catalyzed NT step.

2.5.1 Asymmetric Aziridination Catalyzed by Silver Complexes

Metal-catalyzed, intramolecular asymmetric aziridinations are limited to a few examples of Rh and Cu catalysts; even these cases are restricted to simple disubstituted alkenes. ^{12a,34} Intermolecular versions display similar limitations in terms of scope. ^{7,8,35} The surprising paucity of such methods, given the utility of enantioenriched aziridines as valuable synthetic building blocks, prompted our explorations of silver catalysis to expand the scope of asymmetric aziridination.

Early investigations revealed a tert-butyl-substituted bis(oxazoline) ligand (t-BuBOX) in combination with AgClO₄ could successfully promote asymmetric aziridination of a series of substituted homoallylic carbamates (Scheme 13). 36 This included excellent selectivity for the first reported examples of enantioselective aziridination of 1,1',2-trisubstituted alkenes; however, 1,2,2'-trisubstituted alkenes resulted in a steep reduction in ee. This observation, coupled with determination of the absolute stereochemistry as



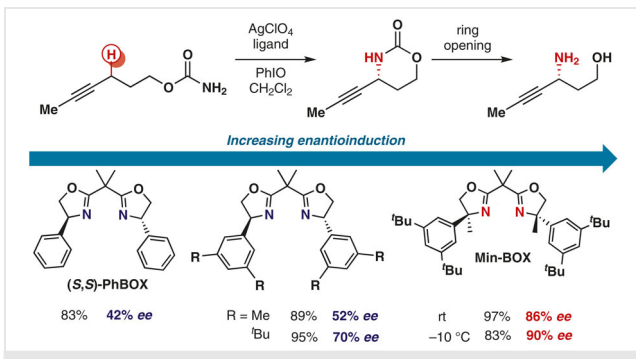
Scheme 13 Enantioselective aziridination examples and stereochemical model

(R,R) enabled us to propose a possible stereochemical model (inset in Scheme 13). The poor ee observed when the proximal alkene carbon R^3 is substituted is rationalized by steric clashing between substrate and catalyst in the transition state. This model is also consistent with the observed tolerance for varied substitution at R^1 and R^2 , along with substitution on the tether.

2.5.2 Asymmetric C–H Insertion Catalyzed by Silver

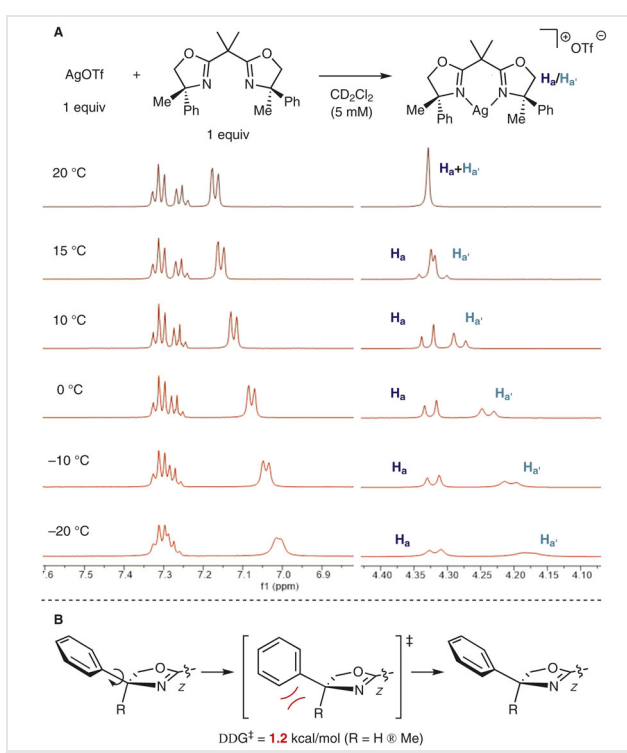
While there are several reports of intramolecular asymmetric NT involving the amidation of benzylic and allylic C-H bonds to furnish chiral γ -amino alcohols,³⁷ to the best of our knowledge, there are no examples of insertion into propargylic C-H bonds to form analogous products. However, there are enantioselective NT reactions of propargylic and unactivated C-H bonds. The work of Zhang and Chang represent the current state-of-the-art in enantioselective C-H insertion via NT. The Zhang group has effectively utilized complex Co-porphyrin catalysts to induce enantioselectivity, 13 due to steric hindrance at the reaction site, while Chang's work on iridium-catalyzed chiral lactam formation takes advantage of noncovalent interactions.³⁸ This has resulted in excellent yields and ee for diverse substrates containing benzylic and challenging unactivated aliphatic C-H bonds. However, neither of these systems can deliver chiral γ-amino alcohols.

Inspired by the success of bis(oxazoline) ligands in achieving regioselective intramolecular C–H insertion and asymmetric aziridination reactions, efforts towards designing a BOX catalyst for intramolecular asymmetric propargylic C–H insertion were undertaken.³⁹ A brief survey of ligands revealed that aryl-box ligands gave moderate *ee* for propargylic C–H bond amidation. Electronic modifications to these scaffolds and attempts to utilize NCIs to improve *ee*



Scheme 14 Structural effects of enantioselectivity of BOX ligands in propargylic C–H amidation

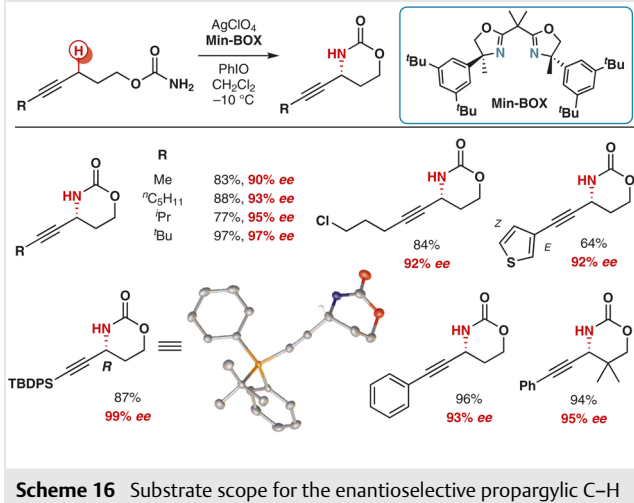
Interestingly, installing a quaternary carbon at the chiral centers of the ligand scaffolds further improved the ee of the reaction. This observation seems to contradict the common understanding regarding the way BOX ligands induce ee.⁴⁰ Interestingly, VT-NMR studies showed substantial chemical shift changes of the diastereotopic protons H_a and $H_{a'}$ and aromatic protons as the temperature decreases (Scheme 15).



Scheme 15 (A) VT-NMR spectra showing the effect of the additional Me substitution in BOX ligands. (B) Increased rotational barrier for Ph group supported by DFT calculations.

These changes in chemical shift were not observed when BOX ligands lacking the fully substituted carbon center were employed. These results implied the presence of the quaternary center imparts a relatively high energy barrier to rotation of the phenyl group, a conclusion that was further supported by computational data. We hypothesized this increased rotational barrier enforces a more restricted conformation in the transition state, which subsequently translates to increased enantioselectivity.

The excellent reactivity of the newly designed Min-BOX ligand, which combines insights resulting from the optimization of the steric profile of the catalyst, was further optimized in terms of temperature to further increase *ee*. Several homopropargylic carbamates gave both good yields and *ee* in the reaction, regardless of the steric profile of the substrate (Scheme 16). Electronic modifications to the substrates were also well-tolerated.



Scheme 16 Substrate scope for the enantioselective propargylic C–H amidation reaction

We envisage these compounds being valuable building blocks for drug and other synthetic targets containing a chiral 1,3-amino alcohol moiety. 1b,c

3 Summary and Perspective

3.1 Future Opportunities and Challenges

Despite the significant progress made by our group and others, many aspects of NT remain challenging. The intramolecular activation of electron-deficient C–H bonds is rare and requires more reactive nitrene species that can display lowered selectivity. Intramolecular asymmetric NT into unactivated and diverse types of allylic C–H bonds that yield nonamide products with broad scope are also lacking. In terms of intermolecular C–H bond amidation, the site- and stereoselective activation of tertiary C–H bonds has yet to be achieved. In addition, many intermolecular strategies

that do not use pre-oxidized nitrogen sources require a large excess of substrate, though significant advances have been made towards this end. While remarkable enantiose-lectivities have been achieved for intramolecular NT involving select nitrene precursors, these products are limited to lactams, pyrrolidines, and a few scattered examples of amino alcohols. Stereoselective intermolecular NT reactions are even more scarce and are mainly reliant on substrate control. Ultimately, a suite of NT catalysts capable of predictable and tunable chemo-, site-, and enantioselective transformations of C-H and C=C bond, either in an intra- or intermolecular manner, would revolutionize the way in which chemists approach the synthesis of valuable amines and late-stage functionalization of natural products and pharmaceuticals to prepare useful analogues.

3.2 Conclusion

In summary, nitrene transfer continues to be a rapidly growing field full of possibilities and challenges. Our group has shown that silver-based catalysts have the unique ability to tackle issues that include tunable chemo-, site-, and stereoselectivity through judicious choice and modification of ligand scaffold. Mechanistic investigations and insight gained from computational studies have enabled us to effectively manipulate the coordination environment and noncovalent interactions in silver complexes to furnish unprecedented catalyst control over nitrene reactivity and sets the groundwork for further improvements in the field.

Funding Information

J.M.S. is grateful to the National Science Foundation (NSF, Grant No. 1664374) for financial support of this research. The Paul Bender Chemistry Instrumentation Center was supported by: Thermo Q ExactiveTM Plus by the National Institutes of Health (NIH, Grant No. 1S10 OD020022-1); Bruker Quazar APEX2 and Bruker Avance-500 by a generous gift from Paul J. and Margaret M. Bender; Bruker Avance-600 by the National Institutes of Health (NIH, Grant No. S10 OK012245); Bruker Avance-400 by the National Science Foundation (NSF, Grant No. CHE-1048642) and the University of Wisconsin-Madison; Varian Mercury-300 by the National Science Foundation (NSF, Grant No. CHE-0342998).

Acknowledgment

Dr. Charles G. Fry and Dr. Heike Hofstetter at UW-Madison are thanked for valuable discussions about NMR equipment and techniques. Dr. Martha M. Vestling of UW-Madison is thanked for help with mass spectrometry characterization.

References

(1) (a) Darses, B.; Rodrigues, R.; Neuville, L.; Mazurais, M.; Dauban,
 P. Chem. Commun. 2017, 53, 493. (b) Lait, S. M.; Rankic, D. A.;
 Keay, B. A. Chem. Rev. 2007, 107, 767. (c) Palchykov, V. A.;

- Gaponov, A. A. Adv. Heterocycl. Chem. **2020**, 131, 285. (d) Ager, D. J.; Prakash, I.; Schaad, D. R. Chem. Rev. **1996**, 96, 835. (e) Tok, J. B.-H.; Rando, R. R. J. Am. Chem. Soc. **1998**, 120, 8279. (f) O'Connell, C. E.; Salvato, K. A.; Meng, Z.; Littlefield, B. A.; Schwartz, C. E. Bioorg. Med. Chem. Lett. **1999**, 9, 1541.
- (2) (a) McIntosh, J. A.; Coelho, P. S.; Farwell, C. C.; Wang, Z. J.; Lewis, J. C.; Brown, T. R.; Arnold, F. A. Angew. Chem. Int. Ed. 2013, 52, 9309. (b) Hyster, T. K.; Farwell, C. C.; Buller, A. R.; McIntosh, J. A.; Arnold, F. H. J. Am. Chem. Soc. 2014, 136, 15505. (c) Prier, C. K.; Zhang, R. K.; Buller, A. R.; Brinkmann-Chen, S.; Arnold, F. H. Nat. Chem. 2017, 9, 629. (d) Yang, Y.; Cho, I.; Qi, X.; Liu, P.; Arnold, F. A. Nat. Chem. 2019, 11, 987. (e) Dydio, P.; Key, H. M.; Hayashi, H.; Clark, D. S.; Hartwig, J. F. J. Am. Chem. Soc. 2017, 139; 1750. (f) Singh, R.; Bordeaux, M.; Fasan, R. ACS Catal. 2014, 4, 546.
- (3) Bommarius, A. S. Annu. Rev. Chem. Biomol. Eng. 2015, 6, 319.
- (4) For select reviews, see: (a) Muller, P.; Fruit, C. Chem. Rev. 2003, 103, 2905. (b) Driver, T. G. Org. Biomol. Chem. 2010, 8, 3831. (c) Chang, J. W. W.; Ton, T. M. U.; Chan, P. W. H. Chem. Rec. 2011, 11, 331. (d) Lu, H.; Zhang, X. P. Chem. Soc. Rev. 2011, 40, 1899. (e) Roizen, J. L.; Harvey, M. E.; Du Bois, J. Acc. Chem. Res. 2012, 45, 911. (f) Gephart, R. T. III.; Warren, T. H. Organometallics 2012, 31, 7728. (g) Dequirez, G.; Pons, V.; Dauban, P. Angew. Chem. Int. Ed. 2012, 51, 7384. (h) Chu, J. C. K.; Rovis, T. Angew. Chem. Int. Ed. 2018, 57, 62. (i) Alderson, J. M.; Corbin, J. R.; Schomaker, J. M. Acc. Chem. Res. 2017, 50, 2147.
- (5) Kwart, H.; Kahn, A. A. J. Am. Chem. Soc. 1967, 89, 1951.
- (6) Breslow, R.; Gellman, S. H. J. Am. Chem. Soc. 1983, 105, 6728.
- (7) Evans, D. A.; Faul, M. M.; Bilodeau, M. T.; Anderson, B. A.; Barnes, D. M. J. Am. Chem. Soc. 1993, 115, 5328.
- (8) Li, Z.; Conser, K. R.; Jacobsen, E. N. J. Am. Chem. Soc. 1993, 115, 5326.
- (9) (a) Espino, C. G.; Wehn, P. M.; Chow, J.; Du Bois, J. J. Am. Chem. Soc. 2001, 123, 6935. (b) Espino, C. G.; Du Bois, J. Angew. Chem. Int. Ed. 2001, 40, 598. (c) Espino, C. G.; Fiori, K. W.; Kim, M.; Du Bois, J. J. Am. Chem. Soc. 2004, 126, 15378. (d) Fiori, K. W.; Du Bois, J. J. Am. Chem. Soc. 2007, 129, 562. (e) Harvey, M. E.; Musaev, D. G.; Du Bois, J. J. Am. Chem. Soc. 2011, 133, 17207. (f) Roizen, J. L.; Zalatan, D. N.; Du Bois, J. Angew. Chem. Int. Ed. 2013, 52, 11343. (g) Bess, E. N.; DeLuca, R. J.; Tindall, D. J.; Oderinde, M. S.; Roizen, J. L.; Du Bois, J.; Sigman, M. S. J. Am. Chem. Soc. 2014, 136, 5783. (h) Chiappini, N. D.; Mack, J. B. C.; Du Bois, J. Angew. Chem. Int. Ed. 2018, 57, 4956.
- (10) (a) Fruit, C.; Robert-Peillard, F.; Bernardinelli, G.; Muller, P.; Dodd, R. H.; Dauban, P. *Tetrahedron: Asymmetry* 2005, 16, 3484.
 (b) Liang, C. G.; Robert-Pedlard, F.; Fruit, C.; Muller, P.; Dodd, R. H.; Dauban, P. *Angew. Chem. Int. Ed.* 2006, 45, 4641. (c) Collet, F.; Lescot, C.; Liang, C.; Dauban, P. *Dalton Trans.* 2010, 39, 10401.
 (d) Lescot, C.; Darses, B.; Collet, F.; Retailleau, P.; Dauban, P. J. Org. Chem. 2012, 77, 7232.
- (11) (a) Fantauzzi, S.; Caselli, A.; Gallo, E. Dalton Trans. 2009, 28, 5434. (b) Lu, H.-J.; Jiang, H.-L.; Hu, Y.; Wojtas, L.; Zhang, X. P. Chem. Sci. 2011, 2, 2361. (c) Lyaskovskyy, V.; Suarez, A. I. O.; Lu, H.-J.; Zhang, X. P.; de Bruin, B. J. Am. Chem. Soc. 2011, 133, 12264. (d) Lu, H.-J.; Li, C.-Q.; Jiang, H.-L.; Lizardi, C. L.; Zhang, X. P. Angew. Chem. Int. Ed. 2014, 53, 7028. (e) Paradine, S. M.; White, M. C. J. Am. Chem. Soc. 2012, 134, 2036. (f) Paradine, S. M.; Griffin, J. R.; Zhao, J.; Petronico, A. L.; Miller, S. M.; White, M. C. Nat. Chem. 2015, 7, 987. (g) Clark, J. R.; Feng, K. F.; Sookezian, A.; White, M. C. Nat. Chem. 2018, 10, 583.
- (12) (a) Dauban, P.; Dodd, R.; Esteoule, A.; Duran, F.; Retailleau, P. Synthesis 2007, 1251. (b) Barman, D. N.; Nicholas, K. M. Eur. J. Org. Chem. 2011, 908. (c) Braga, A. A. C.; Maseras, F.; Urbano,

- J.; Caballero, A.; Diaz-Requejo, M. M.; Pérez, P. J. Organometallics 2006, 25, 5292.
- (13) (a) Li, C. Q.; Lang, K.; Lu, H. J.; Hu, Y.; Cui, X.; Wojtas, L.; Zhang, X. P. Angew. Chem. Int. Ed. 2018, 57, 16837. (b) Lang, K.; Torker, S.; Wojtas, L.; Zhang, X. P. J. Am. Chem. Soc. 2019, 141, 12388. (c) Hu, Y.; Lang, K.; Li, C.; Gill, J. B.; Kim, I.; Lu, H.; Fields, K. B.; Marshall, M.; Cheng, Q.; Cui, X.; Wojtas, L.; Zhang, X. P. J. Am. Chem. Soc. 2019, 141, 18160.
- (14) Hong, S. Y.; Park, Y.; Hwang, Y.; Kim, Y. B.; Baik, M. H.; Chang, S. *Science* **2018**, 359, 1016.
- (15) Cui, Y.; He, C. J. Am. Chem. Soc. 2003, 125, 16202.
- (16) Li, Z.; Capretto, D. A.; Rahaman, R.; He, C. *Angew. Chem. Int. Ed.* **2007**, 46, 5184.
- (17) Beltrán, Á.; Lescot, C.; Mar Díaz-Requejo, M.; Pérez, P. J.; Dauban, P. *Tetrahedron* **2013**, 69, 4488.
- (18) Llaveria, J.; Beltrán, Á.; Sameera, W. M. C.; Locati, A.; Díaz-Requejo, M. M.; Matheu, M. I.; Castillón, S.; Maseras, F.; Pérez, P. J. J. Am. Chem. Soc. **2014**, *136*, 5342.
- (19) Annapureddy, R. R.; Jandl, C.; Bach, T. J. Am. Chem. Soc. 2020, 142, 7374.
- (20) (a) Smith, P. A. S.; Brown, B. B. J. Am. Chem. Soc. 1951, 73, 2435.
 (b) Smith, P. A. S.; Clegg, J. M.; Hall, J. H. J. Org. Chem. 1958, 23, 524. (c) Barton, D. H. R.; Morgan, L. R. Jr. J. Chem. Soc. 1962, 622.
- (21) (a) Lebel, H.; Trudel, C.; Spitz, C. Chem. Commun. 2012, 48, 7799.
 (b) Lebel, H.; Spitz, C.; Leogane, O.; Trudel, C.; Parmentier, M. Org. Lett. 2011, 13, 5460.
- (22) (a) Adams, C. S.; Boralsky, L. A.; Guzei, I. A.; Schomaker, J. M. J. Am. Chem. Soc. 2012, 134, 10807. (b) Weatherly, C. D.; Rigoli, J. W.; Schomaker, J. M. Org. Lett. 2012, 14, 1704. (c) Rigoli, J. W.; Boralsky, L. A.; Hershberger, J. C.; Meis, A. R.; Guzei, I. A.; Schomaker, J. M. J. Org. Chem. 2012, 77, 2446. (d) Liu, L.; Gerstner, N. C.; Oxtoby, L. J.; Guzei, I. A.; Schomaker, J. M. Org. Lett. 2017, 19, 3239.
- (23) (a) Du, J.; Hu, T.; Zhang, S.; Zeng, Y.; Bu, X. CrystEngComm 2008, 10, 1866. (b) Hung-Low, F.; Renz, A.; Klausmeyer, K. K. Polyhedron 2009, 28, 407. (c) Hung-Low, F.; Renz, A.; Klausmeyer, K. K. J. Chem. Crystallogr. 2011, 41, 1174. (d) Zhang, H.; Chen, L.; Song, H.; Zi, G. Inorg. Chim. Acta 2011, 366, 320. (e) Schultheiss, N.; Powell, D. R.; Bosch, E. Inorg. Chem. 2003, 42, 5304.

- (24) Rigoli, J. W.; Weatherly, C. D.; Alderson, J.; Vo, B. T.; Schomaker, J. M. *J. Am. Chem. Soc.* **2013**, *135*, 17238.
- (25) Weatherly, C. D.; Alderson, J. M.; Berry, J. F.; Hein, J. E.; Schomaker, J. M. Organometallics 2017, 36, 1649.
- (26) Dolan, N. S.; Scamp, R. J.; Yang, T.; Berry, J. F.; Schomaker, J. M. J. Am. Chem. Soc. 2016, 138, 14658.
- (27) Luo, Y.-R. Handbook of Bond Dissociation Energies in Organic Compounds; CRC Press: Boca Raton, 2003.
- (28) Scamp, R.; Alderson, J. M.; Phelps, A. M.; Dolan, N. S.; Schomaker, J. M. J. Am. Chem. Soc. 2014, 136, 16720.
- (29) Huang, M.; Corbin, J. R.; Dolan, N. S.; Fry, C. G.; Vinokur, A.;
- Guzei, I. A.; Schomaker, J. M. Inorg. Chem. 2017, 56, 6725.
 (30) Huang, M.; Paretsky, J.; Schomaker, J. M. ChemCatChem 2020, 12, 3076.
- (31) Huang, M.; Yang, T.; Paretsky, J.; Berry, J. F.; Schomaker, J. M. *J. Am. Chem. Soc.* **2017**, 139, 17376.
- (32) Scamp, R. J.; Jirak, J. G.; Guzei, I. A.; Schomaker, J. M. Org. Lett. **2016**. 18. 3014.
- (33) Ju, M.; Huang, M.; Vine, L. F.; Roberts, J. M.; Dehghany, M.; Schomaker, J. M. Nat. Catal. 2019, 2, 899.
- (34) Liang, J.-L.; Yuan, S.-X.; Chan, P. W.; Che, C.-M. Tetrahedron Lett. **2003**, *44*, 5917.
- (35) (a) Subbarayan, V.; Ruppel, J. V.; Zhu, S.; Perman, J. A.; Zhang, X. P. *Chem. Commun.* **2009**, *28*, 4266. (b) Kim, C.; Uchida, T.; Katsuki, T. *Chem. Commun.* **2012**, *48*, 7188.
- (36) Ju, M.; Weatherly, C. D.; Guzei, I. A.; Schomaker, J. M. Angew. Chem. Int. Ed. 2017, 56, 9944.
- (37) (a) Milczek, E.; Boudet, N.; Blakey, S. Angew. Chem. Int. Ed. 2008, 47, 6825. (b) Zalatan, D. N.; Du Bois, J. J. Am. Chem. Soc. 2008, 130, 9220.
- (38) (a) Park, Y.; Chang, S. Nat. Catal. 2019, 2, 219. (b) Wang, H.; Park, Y.; Bai, Z.; Chang, S.; He, G.; Chen, G. J. Am. Chem. Soc. 2019, 141, 7194.
- (39) Ju, M.; Zerull, E. E.; Roberts, J. M.; Huang, M.; Schomaker, J. M. *J. Am. Chem. Soc.* **2020**, in press; DOI: 10.1021/jacs.0c05726.
- (40) (a) Whitesell, J. K. Chem. Rev. 1989, 89, 1581. (b) Rasappan, R.;
 Laventine, D.; Reiser, O. Coord. Chem. Rev. 2008, 252, 702.
 (c) Desimoni, G.; Faita, G.; Jørgensen, K. A. Chem. Rev. 2011, 111, 284.